Research Article
Volume 13:4,2020
DOI: 10.37421/jcsb.2020.13.310

Journal of Computer Science & Systems Biology

ISSN: 0974-7230

Open Access

Evolutionary Dynamics of Microbial Communities in Bioelectrochemical Systems

Lukasz Szydlowski[1], Anatoly Sorokin[2,3], Olga Vasieva[4], Susan Boerner[1], Veyacheslav Fedorovich[1] and Igor Goryanin[1,5,6*]

[1]*Biological Systems Unit, Okinawa Institute of Science and Technology, Japan*

[2]*Institute of Cell Biophysics, Russian Academy of Science, Russia*

[3]*Institute of Physics and Technology, Russia*

[4]*University of Liverpool, United Kingdom*

[5]*The School of Informatics, University of Edinburgh, United Kingdom*

[6]*Tianjin Institute for Industrial Biotechnology, China*

Abstract

Bio-electrochemical systems can generate electricity by virtue of mature microbial consortia that gradually and spontaneously optimize performance. To evaluate selective enrichment of these electrogenic microbial communities, five, 3-electrode reactors were inoculated with microbes derived from rice wash wastewater and incubated under a range of applied potentials. Reactors were sampled over a 12-week period and DNA extracted from anodic, cathodic, and planktonic bacterial communities was interrogated using a custom-made bioinformatics pipeline that combined 16S and metagenomic samples to monitor temporal changes in community composition. Some genera that constituted a minor proportion of the initial inoculum dominated within weeks following inoculation and correlated with applied potential. For instance, the abundance of *Geobacter* increased from 423-fold to 766-fold between -350 mV and -50 mV, respectively. Full metagenomic profiles of bacterial communities were obtained from reactors operating for 12 weeks. Functional analyses of metagenomes revealed metabolic changes between different species of the dominant genus, *Geobacter,* suggesting that optimal nutrient utilization at the lowest electrode potential is achieved via genome rearrangements and a strong inter-strain selection, as well as adjustment of the characteristic syntrophic relationships. These results reveal a certain degree of metabolic plasticity of electrochemically active bacteria and their communities in adaptation to adverse anodic and cathodic environments.

Keywords: Bioelectrochemical systems • Microbial fuel cells • Electrogenic microorganisms • Comparative metagenomics

Introduction

Bio-electrochemical Systems (BESs) refer to microbial communities that either generate electricity, as in Microbial Fuel Cells (MFCs), or utilize electricity, as in Microbial Electrolysis Cells (MECs) [1,2]. BES is a well-known technology allowing simultaneous wastewater treatment and electricity production. BES performance depends on activities of electrochemically-active bacteria (EAB) that form biofilms on anodic surfaces [3]. Various factors account for EAB enrichment: organic substrates, pH, temperature, electrode composition, and electrical potential [2,4-8].

EAB reach maximum power density when reactors operate at near-neutral pH, at ambient temperatures (25-40°C) and are fed with organic loading rates up to 8 g/L COD [9]. However, in most industrial applications it is not feasible to modify the waste stream on the continuous basis, thus the main factor determining EAB enrichment would be anode potential, which determines energy gain for microbial community [10]. Although some studies indicate optimum electrode potentials close to 0 mV in comparison with a standard hydrogen electrode (SHE) [5], based upon thermodynamics of acetate consumption, others have found that the most efficient EAB prefer lower anode potentials [6,11]. Conversely, Zhu and colleagues [12], found no significant difference in EAB community, when a set of anode potentials ranging from -0.25 to 0.81 V *vs.* SHE was applied, although a difference in electrochemical performance was noted, with higher anode potential leading to higher current and power densities. These results are in line with previous studies [13,14], where EAB developing onanodes polarized at 0.748 V and 0.866 V *vs.* SHE yielded highest current densities, although no community studies were performed. On the other hand, Dennis and colleagues [8], found that set anode potentials in the range between 0.3 and 0.8 V *vs.* SHE influences both EAB community and electrochemical performance. Recently, Mohamed and colleagues [15] reported enrichment of electrogenic microbial communities on polarized anodes (~0.2 V *vs.* SHE) and cathodes (~-0.4 V *vs.* SHE) immersed directly in alkaline hotspirngs for 32 days; those communities differed from the ones that colonized non-polarized control electrodes.

Microbial communities used to inoculate BESs were derived mainly from sludge from wastewater treatment plants [6,16,17], aquatic sediments [18], garden compost [14], biogas digestate [19], and various environmental samples [20,21]. EAB are abundant in many environments, such that virtually all environmental inocula can eventually give rise to stable EAB consortia within 60 days. However, further changes and details of community structure are not well understood.

***Address for Correspondence:** Igor Goryanin, The School of Informatics, University of Edinburgh, United Kingdom, Tel: +81- (0)98-982-3420; E-mail: goryanin@gmail.com*

***Rec date:** 23 May 2020; **Acc date:** 03 June 2020; **Pub date:** 10 June 2020*

Previous studies analyzed changes within microbial populations for up to several weeks [19,22,23], and employed mainly 16S sequencing [8,11,24-26], Ribosomal Intergenic Spacer Analysis (RISA) [17] or Denaturing Gradient Gel Electrophoresis (DGGE) [27]. However, these population studies may significantly underestimate microbial diversity, with novel taxonomic groups not detected due to low compatibility with universal primers [28,29]. More complex data has been obtained from pyrosequencing [12] metagenomic [26] and combined metagenomic and metatranscriptomic sequencing [16,30]. In some of the aforementioned studies [27,30], reactors were fed with sucrose, which cannot be metabolized by EABs as efficiently [10] as acetate [4,19,31-33] Sucrose-fed systems develop fermentative communities that do not participate in electron transfer and hence exhibit lower power densities and coulombic efficiencies compared to acetate-fed systems [24,34]. Ishii and colleagues [16] used wastewater, which is complex medium, containing both organic acids as well as carbohydrates. Moreover, the type of inoculum also influences community development. In our previous work, electrogenic communities derived from different sources exhibit different properties in terms of COD consumption, as well as coulombic efficiencies. Therefore, communities present in particular waste streams should already contain some electrogenic bacterial taxa. Nevertheless, the minimal number of EAB is unknown and it remains unclear how quickly they may evolve under different conditions.Thus, complex studies examining long-term community changes across a range of EAB-selective electrode potentials using different inocula are needed.

In this study, we investigated enrichment of EAB in a single-chamber, three-electrode BES. We used an inoculum derived from rice wash process in an awamori distillation plant in Okinawa, Japan. Normalization of conditions among reactors utilizing acetate feeding provided selection pressure for metabolic pathways relevant to electrogenic respiration. Application of potentials ranging from -50 mV to -350 mV *vs.* Ag/AgCl (147 mV to -153 mV *vs.* SHE) on anodes and compositional and functional changes in the resulting bacterial communities were tracked using detailed metagenomics.

Experimental Procedures

Reactor setup and operating conditions

Four reactors (M1-4) were designed as follows: 1.2 L chamber with an anode consisting of 6 carbon-fiber strips (Zoltec) 3 × 10 cm connected with titanium wire (Kojundo chemical laboratory), a cathode consisting of 6 carbon-fiber strips (Zoltec) 3 × 10 cm connected with titanium wire, and a reference electrode (Radiometer Analytical, Hach). Top part was the only mobile element, sealed with rubber to prevent leakage. Additionally, one control reactor (M5) consisted only of one set of 6 carbon-fiber strips (Zoltec) 3 × 10 cm connected with titanium wire and reference electrode (Radiometer Analytical, Hach), and was operated in open circuit mode (Figure S1 for schematic view). A four-channel potentiostat (UniChem) was connected to each reactor with stainless steel clips and potential differences of -50 mV, -150 mV, -250 mV, -350 mV *vs.* Ag/AgCl (147 mV, 47 mV, -53 mV and -153 mV *vs.* SHE) were applied to anodes M 1-4A, respectively. Each reactor was inoculated with rice wash water (1.2 L), derived from Mizuho Shuzo awamori distillery (Naha, Okinawa) and incubated for 2 weeks at room temperature (23°C), after which the liquid was replaced with an equal volume of the following autoclaved medium: 0.05 M phosphate buffer (pH 6), 200 mg/L $CaCl_2{\bullet}2H_2O$, 250 mg/L $MgCl_2{\bullet}6H_2O$, 500 mg/L NH_4Cl, sodium acetate 2g COD/L [33]. COD concentration was measured using a Hach COD kit (Hach, USA). The medium was replaced 6 times at 2-week intervals, yielding a total operating time of 12 weeks. Additionally, 50 mL of liquid fraction and one strip of each electrode (1 × A and 1 × C from M1-4 and 1 × A from M5) were collected with every change of medium. These were used for DNA extraction and SEM analysis.

Microscopic imaging

Samples for microscopic imaging were taken simultaneously with the DNA samples and processed with osmium, as follows [35]: upon removal from the anode compartment, the samples were immediately cut by knife, and fixed by 1% Osmium diluted with 0.2 M Cacodylate (Wako) buffer 30 min. The samples were then washed three times with RQ water and dehydrated stepwise with a graded series of ethanol solutions (70, 80, 90, 95 and three times 100%). The electrode samples were finally critical-point dried with tert-butyl ethanol and sputter coated with a thin layer of gold. The samples were analyzed by a scanning electron microscopy (SEM) (JSM-7900FJEOL).

DNA extraction and library preparation

DNA was extracted using TRIzol (Life Technologies) and additional samples were subjected to Maxwell extraction (GMO pure food kit, Maxwell) using an automated RSC system (Promega). Samples with sufficient amounts of DNA were subjected to Illumina sequencing (48). Remaining samples (32) were subjected to 16S sequencing. DNA libraries were constructed using Nextera XT kit (Illumina) and sequencing was performed on MiSeq platform (Illumina, San-Diego, CA, USA). Samples were uploaded to MG-RAST (mgp81854 for 16S, mgp82844 for metagenomes) and SRA (PRJNA592260). We were unable to collect data from 3 cathodic samples (Table S1).

Bioinformatic analysis

Whole-genome sequences and 16S sequences were analyzed using a custom-developed pipeline, as described elsewhere [36], which carried out taxonomic analysis using Kaiju [37], as well as functional analysis using PALADIN (only applicable to metagenomes) [38]. Results of PALADIN analysis for anodes M1 and M4 can be found in the Supplementary material (Table S3). Compositional analysis of communities was performed in R version 1.4.0 [39] with package compositions [40]. Relative abundance was represented as composition with absolute geometry (rcomp). To combine 16S and metagenomic sequences, datasets from Kaiju and MG-RAST were manually curated (a more detailed description can be found at https://github.com/lptolik/ASAR). One-way ANOVA was conducted to determine the significance of differences in abundance of *Geobacter* between M1A, M2A and M4A for the period between week 8 and 12. For visualization purposes, the five most abundant genera in the inoculum and five most abundant genera in Week 12 were selected. All other genera were included in the "Other" group. The R script employed is described in Orakovet al. [36]. The analysis of metagenome diversity was carried out using R version 3.6.0 (need to add ref here and below).Multidimensional scaling was performed with the "dist" and "cmd scale" functions, and MDS (PCoA) plots were generated with ggplot2. For PERMANOVA, we used the "adonis" function in the vegan package [41-49].

Results

Conditions within reactors

The single-chamber, 3-electrode BES reactors (M1-M4) were connected to a potentiostat to apply fixed potentials (147 mV to -153 mV *vs.* SHE) to the working electrodes (anodes). We also measured potentials observed (792 mV to 1182 mV *vs.* SHE) on counter electrodes (cathodes) in the first week of experiment. In addition, we prepared one reactor (M5) with only one set of electrodes to operate under open circuit potential (OCP) (Table 1). Our BESs were designed to develop electroactive biofilms, with high volume-to-electrode surface ratios in order to minimize nutrient limitations. Thus, after setting a constant potential, the potentiostat maintained current flow automatically and we did not measure current. One channel of the potentiostat, attached to reactor poised at -250 mV, exhibited an overload error after 8 weeks of operation, resulting in turbidity. This caused a shift in

community structure (Figure S2); hence, we excluded this reactor from our analysis.

Table 1. Potentials (measured with Ag/AgCl reference electrode in saturated KCl; +0.197 mV *vs.* SHE) *vs.* SHE on anode (A) and cathode (C) of each reactor. a) Electrode potential measured in the control (OCP) reactor after every 2 weeks. *Potentials measured in the first week of experiment only † Around week 8, we experienced a technical fault in M5 reactor, resulting in overcharge of the reactor, which caused a shift in the microbial community; results for this reactor are in supplementary material, Figure S2.

Reactor	Anode potential mV (*vs.* SHE)	Cathode potential* mV (*vs.* SHE)
M1	-50 (147)	595 (792)
M2	-150 (47)	775 (972)
M3†	-250 (-53)	885 (1082)
M4	-350 (-153)	985 (1182)
M5	0 to -530 (0 to -333)[a]	NA

Community analysis

Samples were collected every two weeks from anodes (M1-5A), cathodes (M1-4C) and planktonic (free swimming) fractions (M1-5P). Microscopic imaging (Figure 1) revealed that anodes from M1-M4 reactors developed communities that formed thick biofilms (Figures 1a-1c), and they were more abundantly populated than cathodes (Figures 1e-1g). No comparable community formed on electrode strips in M5 (Figure 1d), due to its OCP mode. Negative charge accumulation on the electrode eventually inhibited microbial growth (Table 1).

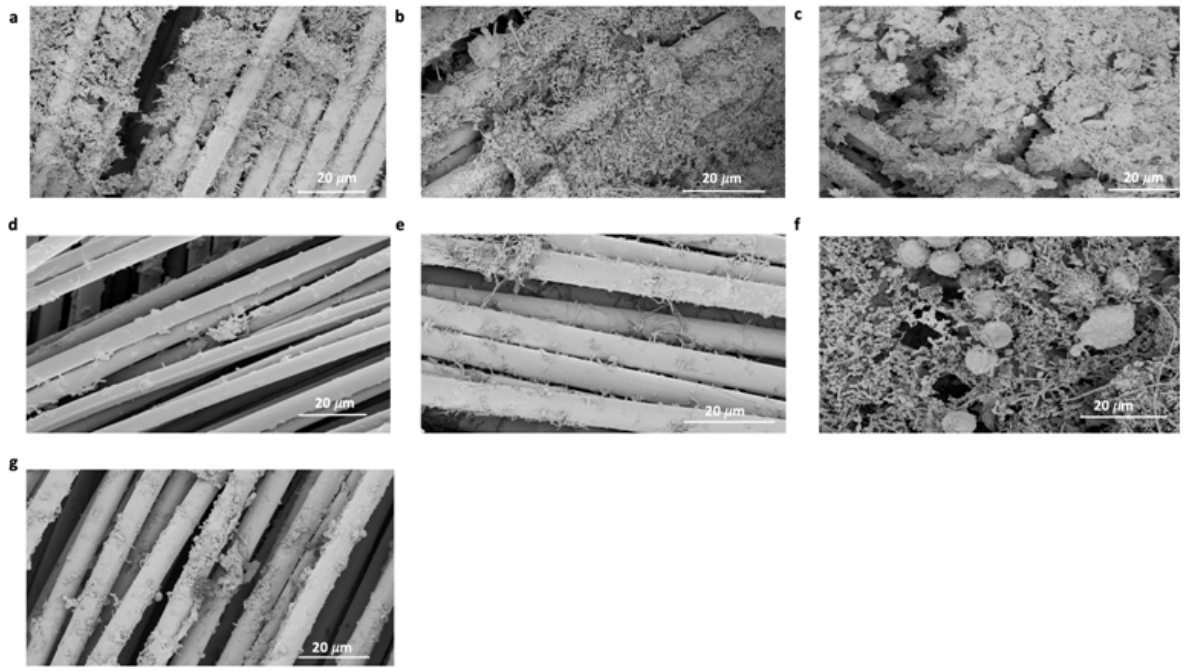

Figure 1. SEM images of electrodes from a) M1A (anode), b) M2A (anode), c) M4A (anode) d) M5A (anode) e) M1C (cathode), f) M2C (cathode) and g) M4C (cathode) after 12 weeks of operation.

Taxonomic analysis of anodes

We analyzed organismal abundances on each anode (Figure 2) during the 12-week operation and compared them with initial community compositions (Table S2). Although rice inoculum is nutrient-rich, the abundance of electrogenic taxa were very low, with *Geobacter and Shewanella* spp., two of the most efficient EABs, comprising less than 0.09% and 0.02% of the total communities, respectively. Enrichment data indicated that the abundance of *Geobacter* spp. rapidly increased over the first 6-8 weeks under poised anode potential (M1-4). Between 8 and 12 weeks, *Geobacter* growth rates plateaued and the change in abundance of *Geobacter* after 12 weeks was 766-fold, 598-fold and 423-fold in M1A, M2A and M4A, respectively, whereas in M5A it only increased 1.2-fold. The relative abundance of *Geobacter* was significantly higher (ANOVA, $p < 0.05$) in M1A at -50 mV and decreased with decreasing potential. After 12 weeks of operation, the abundance of *Shewanella* remained unchanged in all reactors. Control reactor M5 showed an oscillating pattern of the most abundant genera *Methanosaeta*, *Methanobacterium*, and *Acinetobacter*, with an opposite oscillation pattern of *Prevotella* (Figure 2d), although the changes are not as significant as in the other reactors. With regard to generic abundance differences between the reactors, for M1A, *Geobacter* was the only genus with an abundance over 1% after 12 weeks' operation. M2A had 2 such genera (*Geobacter* and *Denitrovibrio*) and in reactor M4 and M5 anodes, the number of significantly abundant (i.e., > 1%) genera reached 10. In the initial inoculum, 5 genera showed abundances >1%.

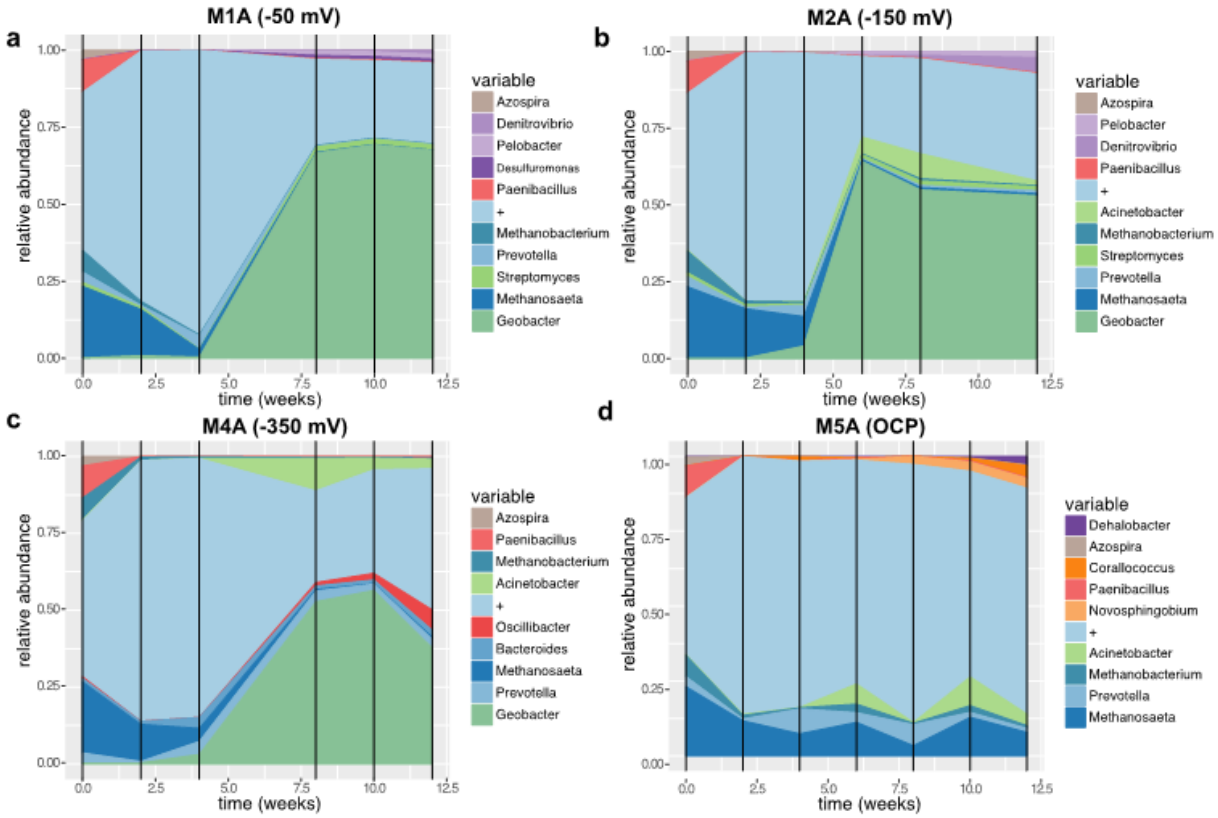

Figure 2. Relative abundances of anodic dominant genera collected from a) M1A, b) M2A, c) M4A and d) M5A during the experiment. Colors represent specific taxonomic groups, "+" refers to all other organisms.

Taxonomic analysis of cathodes

On the M1 and M2 cathodes, the most abundant organisms were methanogenic archaea (Figures 3a and 3b); however, a proportion of *Methanosaeta*, the most abundant methanogenic genus from the initial inoculum, decreased during the course of the experiment with the subsequent growth of *Methanobacter* spp.

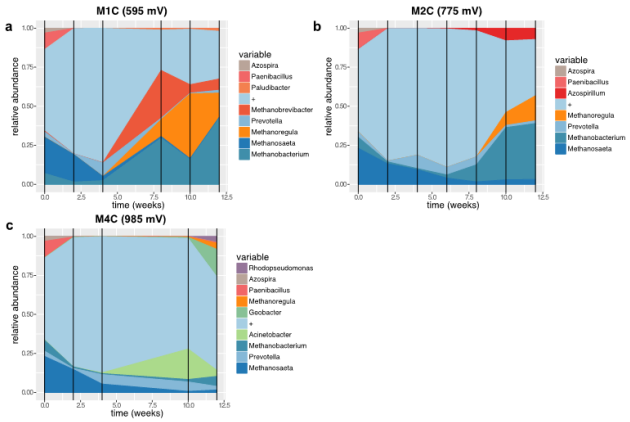

Figure 3. Relative abundances of cathodic dominant genera collected a) M1C, b) M2C and c) M4C during the experiment. Colors represent specific taxonomic groups, "+" refers to all other organisms.

The growth of the latter was in turn inversely correlated with that of *Methanoregula*. Unexpectedly, *Geobacter* was the most abundant genus on M4C, reaching a peak abundance of 16%, 12 weeks after inoculation, a level four times higher than that of the next most abundant genus, *Methanobacterium* (Figure 3c). *Geobacter* remained scarce on the M1 and M2 cathodes (< 0.1%), not exceeding its abundance in the inoculum. On the M4 cathode, a rapid increase in *Geobacter* abundance after 10 weeks was accompanied by a concomitant decrease of *Acinetobacter* from 25% to 2.5% (Figure 3c).

Taxonomic analysis of planktonic communities

In the case of planktonic samples (Figure 4), in M1P, a pattern of sudden growth around week 8, similar to that observed on M1A (although with much lower abundances) was observed with the genera, *Pelomonas*, *Paludibacter*, and *Bacteroides*.

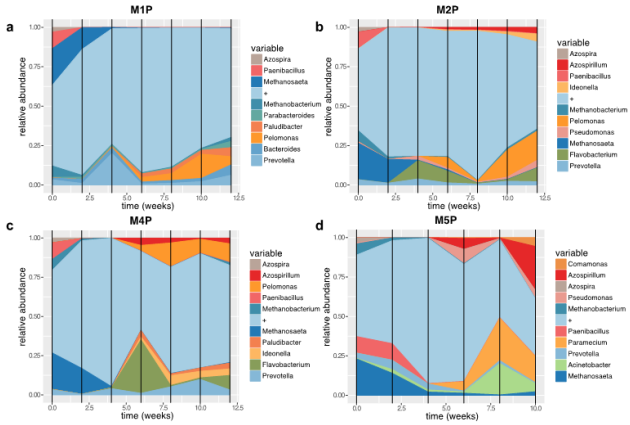

Figure 4. Relative abundances of planktonic dominant genera collected from a) M1P b) M2P c) M4P and d) M5P during the experiment. Colors represent taxonomic groups, "+" refers to all other organisms.

In all planktonic samples, *Methanosaeta*, the most abundant genus in the inoculum (Table S1), decreased within the first weeks of operation, as did *Porphyromonas and Azospirillum*. The proportion of *Pelomonas*, a genus comprising 0.01% of the initial community, rose to about 20% of the total planktonic community in M2 after 12 weeks. In M5P, abundances did not

reflect the initial community profile, as *Methanosaeta* decreased within 4 weeks from 24% to ~1%, whereas *Azospirillum* abundance reached ~25%. *Geobacter* abundance was 6.54%, 1.92%, 4.27% and < 0.05% in M1, M2, M4 and M5 planktonic communities, respectively.

Diversity of metagenomes

We used multidimensional scaling (Principal Coordinates Analysis, PCoA) to look at how the communities clustered based on sample type (initial sludge, anode, cathode, plankton and OCP) at both the genus level (Figure 5a) and functional levels (Figure 5b) after 12 weeks. Significant differences were found for both levels, with 72% of the distance variability due to sample-type and applied potential at the genus level (Figure5a, p-value 0.01), and 65% (Figure 5b, p-value 0.04) at the functional level. We can thus observe that similar communities formed on different parts of the reactor (anodes, cathodes, plankton), cluster to each other and are all being quite different from the initial inoculum.OCP control (both anode and plankton) also diverge from the initial community.

We also compared the percentage of unclassified reads (at the generic level) from each metagenome to that from the initial inoculum (FigureS3). Results indicate almost a 2-fold increase of unclassified taxa after 12 weeks in all sampled metagenomes, with the highest being reported in M4P (34.9%), followed by M1P (31.9%) and M5P (30.0%), with 17% of unclassified genera in the initial inoculum.

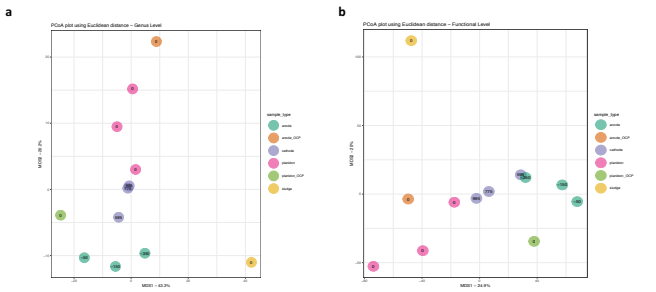

Figure 5. PCoA plots based on a) taxonomy b) function. Values correspond to potentials observed in each compartment that were presented in Table 1. 0 potential corresponds to all planktonic and M5A (OCP control).

Functional overview of metagenomes

Functional analysis of genomic features with the highest differential abundancies between the metagenomes also revealed changes in functions mapped to genomes that were identified via PALADIN analysis. *Methanosaeta* functions were predominant in the initial communities and the M5 reactor, where they ranked in the top 200 by read count (Tables S3 and S7, respectively). *Geobacter*f unctions dominated the ranked lists for the M1, M2, and M4 reactors. To gain a deeper understanding of the communities, we compared abundances in greater detail and ranked the top 200 *Geobacter* functions from each reactor (Supplementary Tables S3-S7). The rank of each gene was established in relation to the normalized abundance of its mapped reads (See Methods for a gene/function abundance calculation) for each species. The function with the highest number of mapped reads was assigned a rank of 1. Functions with lower numbers of mapped reads had lower ranks with larger assigned values. The main abundance trend defined by the taxonomic analysis, correlates with the occurrence of *Geobacter*spp. in reactors, with counts for almost all mapped genes decreasing in the order M>M4>M2>M5. However, we also noticed changes in ranks of several *G.metallireducens* and *G.sulfurreducens* genes that may reflect changes in the proportion of these functionally significant genes in *Geobacteraceae* populations in different reactors. A comparison of M4A to M1A revealed that 14 genes increase and 17 genes decrease in rank in M4A with respect to M1A (Figure 6). An increase in rank order suggests potentially favorable genomic changes and may help to identify species-specific significant functions for specific reactor conditions. Interestingly, the results of such a comparison of *Geobacter* fractions at the M1 and M4 metagenomes (Figure 6) suggests a positive selection of bacteria for functions/genes involved in electrogenic metabolism. Metagenomic changes in *G. sulfurreducens* were related to genes encoding ATP synthase, NADH-quinone oxidoreductase, and the acetate utilization pathway, with 2-fold, 1.8-fold, and 1.5-fold rank increases in M4A compared to M1A. Conversely, *G. sulfurreducens* genes encoding ATPase (*prkA*), citramalate synthase (*cimA*), sodium symporter (*aplC*), aldehyde dehydrogenase (*aldh*), and Fe-S binding protein increased 4-fold, 2.02-fold, 2-fold, 1.52-fold, and 1.51-fold in rank in M1A, respectively. Changes in the *G. metallireducens* metagenome included a wide range of functions involved in conductive pilin assembly (*pilB*), flagella biosynthesis regulation (*fgrM*), pyruvate metabolism (*leuA*), electron transfer (*nuoB/C/G/L and por*), utilization of ammonia (*carb-1*) efflux pump (*cusA*), and aspartokinase (*asd-1*) between 2-fold and 1.5-fold in M4A, whereas periplasmic Ni-Fe dehydrogenase (*hybL*) and NADH-quinone oxidoreductase (*nuoD*) show 1.95 and 1.76-fold increase in M1A.

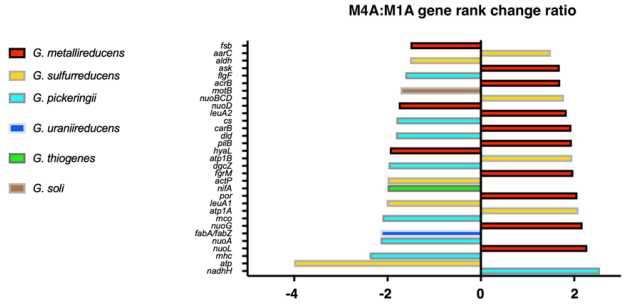

Figure 6. Rank change ratio between M4A and M1A. Colours represent hits with the highest match to one of *Geobacter* spp. Fold change ratio 1.5 was chosen as a threshold. Represented genes are as follows: *fsb*, Fe-S binding protein; *aarC*,Succinyl:acetate coenzyme A transferase ; *aldh*, aldehyde dehydrogenase; *ask*, aspartokinase; *flgF*, flagellar basal-body rod protein; *acrB*, Efflux pump, RND family, inner membrane protein; *motB*, flagellar basal body stator protein; nuoBCD, NADH-quinone oxidoreductase subunit B/C/D (EC 1.6.5.11); *leuA2*, 2-isopropylmalate synthase (EC 2.3.3.13); *cs*,type I citrate synthase (EC 2.3.3.1); *carB*, Carbamoyl-phosphate synthase; *dld*, Dihydrolipoyl dehydrogenase (EC 1.8.1.4); *pilB*, Type IV pilus biogenesis ATPase; *hyaL*, Periplasmically oriented, membrane-bound [NiFe]-hydrogenase; *atp1B*, ATP synthase subunit beta (EC 3.6.3.14); *dgcZ*, Diguanylate cyclase; *fgrM*, Flagellar biogenesis master sigma-54-dependent transcriptional regulator; *actP*, Sodium/solute symporter family protein; *nifA*, Nif-specific regulatory protein; *por*, Pyruvate-flavodoxin oxidoreductase; *leuA1*, (R)-citramalate synthase (EC 2.3.1.182); *atp1A*, ATP synthase subunit alpha; *mco*, multicopper oxidase; *nuoG*, NADH dehydrogenase I, G subunit; *fabA/fabZ*, Beta-hydroxyacyl dehydratase; *nuoA*, NADH-ubiquinone oxidoreductase subunit 3; *nuoL*, NADH dehydrogenase, subunit L; *mhc*, multiheme cytochrome; *atp*, ATPase; *nadhH*, NADH-quinone oxidoreductase subunit H (EC 1.6.5.11).

Genes from the *Geobacteraceae* (*G. pickeringii*, *G. uraniireducens*, *G. thiogenes*, and *G.soli*) mostly increased in rank in M1A, with outer membrane multiheme cytochrome c (*omc*), NADH-ubiquinone oxidoreductase (*nuoA*), β-hydroxyacyl dehydratase (*fabA/Z*), multicopper oxidase (*ompB*), Nif-regulatory protein (*nifA*) exhibiting more than a 2-fold increase in rank, as well as dihydrolipoyl dehydrogenase (*lpdA*), type I citrate synthase (*gltA*), and flagellar components (*motB*, *flgEF*), which exhibited 1.82, 1.81 and 1.7-fold shifts in rank, respectively. In M4A, a 2.55-fold rank increase was observed for the NADHquinone oxidoreductase gene (*nuoH*) from *G. pickeringii*.

In all planktonic samples, as well as in the initial community, top ranked genes are those involved in genome rearrangement (transposases, reverse transcriptases and endonucleases, see Tables S3-S7), which indicates selective pressure for adaptation to a more competitive environment.

Discussion

Abundance of *Geobacter* spp. at anodes is directly proportional to the applied voltage

Rice wash is usually rich in methanogens [50], which are parasitic to the EABs in terms of electron use, therefore we were interested in conditions that would promote growth of ofEAB over methanogenic species. *Geobacter* is a well-characterized genus of EAB that populates BES anodes abundantly [32]. It can comprise ≤ 99% of bacterial communities isolated from BES electrodes operating at the lowest potential [6,12], but inother studies [51] its abundance increases with increased anode potential. Our work indicates that the abundance of *Geobacter* increases at anodes with increasing applied potential, meaning that as the electrode potential increases, *Geobacter* competes more effectively with other genera in the community. It is probably due to the fact that BESs with anodes poised at lower potentials need to have higher resistance to maintain such potential. Resistance load is known to have a significant impact on EAB development [7,16,21,24,25,34,52,53], and thus should be adjusted based throughout EAB biofilm development, e.g., via maximum power point tracking algorhytms [22]. The fact that the resistance load became suboptimal during our experiment, may be indicated by the decrease of *Geobacter* abundance in M2A after 6 weeks of rapid growth, when *Geobacter* abundance was over 2 times higher than in M1A and M4A (Figure 2). In M1A the decrease in week 12, may indicate the resistance becoming limiting factor for the *Geobacter*growth at this stage, whereas in M4A the effect of resistance may be observed in overall lower *Geobacter* abundance than in other anodes.

In contrast to *Geobacter, Shewanella* did not increase in abundance under aforementioned conditions, even though it is also able to respire using electrode as terminal electron acceptor. In this case, however, the lack of abundance increase is likely due to the fact that *Shewanella* primarily utilizes lactate as a carbon source [54,55].

Our abundance results contrast with those of Ishii et al., [25], in which the highest abundance of *Geobacter* spp. In acetate-fed, set-potential reactors was observed when anodes were held at -50 mV *vs.*SHE (-247 mV *vs.* Ag/AgCl), whereas in our study the highest abundance was observed on anodes poised at 147 mV *vs.* SHE (-50 mV *vs.* Ag/AgCl). However, abundances from our study resemble those reported by Dennis et al. [8], and Ishii et al. [30] where highest *Geobacter* abundance was observed on anodes poised at 300 mV and 100 mV *vs.* SHE, respectively. Also, the low initial population of *Geobacter*in the inoculum (Table S2) may explain the slower growth of *Geobacter* spp. At M4 compared to M1 and M2 and overall lower *Geobacter* abundance when compared to Zhu et al. [12] study. Ishii et al. [56] also found different abundance of anodic *Geobacteraceae* species, depending on the initial inoculum. Although periodic metagenomic sequencing reveals changes in the most abundant genera, it also indicates a large number of potentially undetected bacterial taxa. Changes in this community, as well as interactions among the most abundant EAB, will remain enigmatic, however, until genome assembly and isolation methods are improved to identify and characterize new strains.

Presence of *Geobacter* spp. at cathodes

Apart from the *Geobacter* presence at anodes, *Geobacter* also dominated the M4 cathode community after 12 weeks, although it was scarcely present at other cathodes (0.06% and 0.07% in M1 and M2 cathodes, respectively) as well as at the M5 electrode (0.1%), being close to the inoculum abundance (0.08%). Such an increase in *Geobacter* spp. abundance in compartments with opposite conditions reflects its ability to both donate and accept electrons in association with electrodes [18,57]. However, *Geobacter* was not found at cathodes in other studies [19], which may reflect competition with different bacterial taxa, as well as differences in operating conditions, initial community structure, etc. Moreover, rank shifts of flagellar biosynthesis genes demonstrate ongoing colonization of new environmental niches by *Geobacter* spp. Recently, Rittmann and Asce [2] concluded that the best-performing EAB has the lowest anode potential, but noted that such conditions are in fact stressful to the bacteria. Perhaps the M4 cathode offered less deleterious conditions for *Geobacteriae* growth. The continuous decrease of methanogenic archaea at the M4 cathode may hint at competition for electrons with *Geobacter* spp., a known electrotroph. There is, however, no evidence of rank shifts in genes involved in hydrogenotrophicmethanogenesis, such as hydrogenase or methyl coenzyme M reductase. Microscopic observations (Figures 1e-1g) suggest some other relationship between *Geobacter* and methanogens in the cathodic community, for example electromethanogenesisvia direct interspecies electron transfer [58].

Functional analysis and evidence of differential selection pressure on *Geobacter* at low electrode potentials

We were intrigued by the dependence of observed genomic shifts in *Geobacter* metabolic functions on reactor conditions. The changes themselves, relevant to the main pathways of electrogenic organisms in MFCs, suggest that bacterial genomes evolve rapidly due to metabolic competition. Acetate metabolism is central to the metabolism of *G. sulfurreducens* under electrogenic conditions [21,32]. This metabolic feature allows these bacteria to dominate anodic communities if acetate is provided or generated by other members of the syntrophic bacterial community (e.g., *G. metallireducens*). Interestingly, *G. sulfurreducens* functions required for acetate utilization (*ato*) were the only ones from this species that strongly changed rank at lower anodic potential (M4), with aldehyde dehydrogenase rank decreasing (Figure 6). Acetate utilization by *G. sulfurreducens* may be supported by a syntrophic association with *Pelobacter* spp. [59], and enrichment of this genus was observed on anodes M1 and M2 (Figures 2a and 2b). Though acetate was provided in the medium, local interactions between bacteria and bacterial clusters may be significant. Sequences corresponding to ATP synthase subunits also increased in abundance in M4A, with a 4-fold decrease in ATPase (Figure 6), suggesting higher pressure for energy generation.

At the same time, adaptation and evolution of highly electrogenic *G. Metallireducens* at M4 seems to proceed due to a requirement for conductive pili, respiratory NADH dehydrogenases, and pyruvate metabolism, which increase in rank at M4A (Figure 6). NuoL, for which metagenomic rank changed most at the M4 anode compared to M1A, is responsible for the reverse electron transfer and H^+/e^- stoichiometry [60], which may be important for balancing electron flow between NAD^+ and ferredoxin pools. PilB is an ATPase required for polymerization of conductive e-pili [61], and *pilB* mutants are reported to generate lower current and form thinner biofilms [62]. Additionally, it was observed by Ishii et al. [30] that *pilA* expression increased at lower surface potential. Change in *pilB* expression has not been reported in the aforementioned study, although it could be a result of a normalization procedure: with an increase in the abundance of DNA reads, changes in abundance of RNA reads/expression could not be observed.

Flagellar response regulator (*fgrM*), which increased in rank in M4A, regulates flagellar growth, a known feature of *G. metallireducens* when grown with an insoluble Fe (III) source. This feature corresponds to increased motility of cells when Fe (III) sources are sparse. Cells can store electrons in their numerous cytochromes, acting as capacitors, so that they can discharge them upon the next available Fe (III) cluster. Similarly, lower surface potential of the anode in M4A could lead to formation of dispersed local spots for electron release. Thus, *G. metallireducens* cells with regulated expression of flagella proteins could possess higher and more ordered motility, which, together with the higher capacity to polymerize e-pili by PilB, should give them an advantage over competitors.

This study shows a decrease in rank of genes belonging to other taxa (*G. pickeringii*, *G.uraniireducens*, *G. thiogenes* and *G.soli*) at lower surface potential (Figure 6b). Citrate synthase (*G. pickeringii*), a proposed indicator of

Geobacter aceaemetabolic activity [18] decreased almost 2-fold at M4A. Also, genes encoding components of EET, such as multiheme c-type cytochromes are lower in rank at M4A (Figure 6b). Upregulation of multiheme c-type cytochromes' expression has been observed in *G. sulfurreducens* during current generation [63,64]. Although no metatranscriptomic data has been obtained, the rank decrease of MH-cytCs-encoding genescorrelates with the limited capacity of *G. pickeringii* to adapt to low surface potential, as their electrochemical activity was reported for rather more positive redox potentials, whereas potentials below -0.1 *vs.* SHE trigger CbcL-dependent system [30,64], which is not present in *G. pickeringii*.

We conclude that the comparative rank measurement gives a better estimate of a functional genomic shift for a particular metagenome in relation to a reactor condition, which is not surprising when one takes into account that ranks are known to be a robust characterisation of the population for analysis of covariance [65,66]. The rank transformation has been widely used since Charles Spearman defined the correlation coefficient in 1904 and more recently it has been adapted in metagenomics studies of microbial communities [67]. Certainly, gene abundance cannot be taken as an unequivocal reflection of activity levels of relevant functions in bacterial metabolism under different conditions. However, we suggest that genomic rearrangements represent responses to specific functional requirements. Genes may be retained or even propagate in a population if they enhance organismal fitness. Increasing abundances of bacterial strains bearing advantageous genes may also explain the observed phenomenon. As shown in the case of *pilB* gene, analysis of gene ranks derived from metagenomics analysis can complement expression studies.

The importance of unknown organisms in a functional overview of these metagenomes

The presence of unclassified taxa indicates an increase in abundance of unknown organisms upon inoculation into BES reactors. Our results (Figure S3) do not align with other works [8,25], in which unclassified taxa in the inoculum contained comparable numbers of unclassified reads, but only several percent of unclassified organisms were identified in sampled electrodes. The discrepancy between the two studies may be due to the difference in sampling and sequence processing methods. Such discrepancies were also reported in a later study by Ishii et al. [30], where lower diversity was reported in the same samples when only metagenome binning was employed. The abundance of novel unidentified organisms suggests the existence of novel electrogenic microorganisms, as in the case of *in situ* enrichment of EAB from alkaline hot springs [15]. Such organisms may not necessarily be as efficient in EET as *Geobacter* spp.; hence the term "weak electricigens" [68], but they may nonetheless provide useful insight into the divergence of EET mechanisms. However, since their increases do not follow electrode potential, the presence of so many unclassified organisms is perhaps more dependent on the inoculum than the reactor conditions.

Conclusion

This work presents the dynamic nature and complexity of microbial community within MFC reactors. We observed selection of the EAB, which constituted the minor proportion of the initial inoculum, but within the course of weeks dominated the community. We have also noticed metabolic changes between the different species of the most dominant EAB-*Geobacter* that suggest syntropic relationship towards the most efficient nutrient usage upon challenging conditions (anode potential), which could be limiting factors at certain timepoint, given the resistance associated with constant anode potential. We also determined that under certain electrode potential threshold, *Geobacteriae* may start colonizing cathodes, which indicates its rapid adaptation to environment with reversed electron flow, possibly leading to electro-methanogenesis via DIET. Furthermore, we present a novel method of combining 16S and WGS to further study taxonomic compositions of complex MFC community. Although, periodic metagenomic sequencing reveals the changes within the most abundant genera, it also indicates a large number of yet undiscovered bacterial taxa, as well as ongoing genome rearrangements, as indicated by high abundance of transposases and reverse transcriptases. Changes within this community, as well as their interactions within the most abundant EAB will remain unknown, however, until the genome assembly and isolation methods help to identify and characterize new strains.

Acknowledgement

This research was supported by Okinawa Institute of Science and Technology Graduate University. We thank Dr. Larisa Kiseleva for collecting electrode and plankton samples and Dr. Toshio Sasaki for preparing SEM specimens.

Conflict of Interest

The authors declare no conflict of interest.

References

1. Santoro, Carlo, CatiaArbizzani, Benjamin Erable, and IoannisIeropoulos. "Microbial fuel cells: from fundamentals to applications. A review." *J Power Sourc* 356 (2017): 225-244.
2. Rittmann, Bruce E. "Ironies in microbial electrochemistry." *J Environ Eng* 143 (2017): 03117001.
3. Allen, Robin M, and HPeterBennetto. "Microbial fuel cells: electricity production from carbohydrates." *App Biochem Biotech* 39 (1993): 27-40.
4. Logan, Bruce E, Bert Hamelers, René Rozendal, and Uwe Schröder, et al. "Microbial fuel cells: methodology and technology." *Environ SciTech* 40 (2006): 5181-5192.
5. Aelterman, Peter, Stefano Freguia, Jurg Keller, and Willy Verstraete, et al. "The anode potential regulates bacterial activity in microbial fuel cells." *App Microbio Biotech* 78 (2008): 409-418.
6. Torres, César I, Rosa Krajmalnik-Brown, PrathapParameswaran, and Andrew Kato Marcus, et al. "Selecting anode-respiring bacteria based on anode potential: phylogenetic, electrochemical, and microscopic characterization." *Environ Sci Tech* 43 (2009): 9519-9524.
7. Logan, Bruce. "Exoelectrogenic bacteria that power microbial fuel cells." *Nat Rev Microbio* 7 (2009): 375-381.
8. Dennis, Paul G, Bernardino Virdis, Inka Vanwonterghem, and Alif Hassan, et al. "Anode potential influences the structure and function of anodic electrode and electrolyte-associated microbiomes." *Scientific Reports* 6 (2016): 39114.
9. Velvizhi, Gokuladoss, and Venkata Mohan. "Electrogenic activity and electron losses under increasing organic load of recalcitrant pharmaceutical wastewater." *Int J Hydrog Energy* 37 (2012): 5969-5978.
10. Schröder, Uwe. "Anodic electron transfer mechanisms in microbial fuel cells and their energy efficiency." *PhyChem* 9 (2007): 2619-2629.
11. Ishii, Shun'ichi, Kazuya Watanabe, SoichiYabuki, and Bruce E. Logan, et al. "Comparison of electrode reduction activities of *Geobacter* sulfurreducens and an enriched consortium in an air-cathode microbial fuel cell." *App Environ Microbio* 74 (2008): 7348-7355.
12. Zhu, Xiuping, Matthew D Yates, Marta C Hatzell, and Hari Ananda Rao, et al. "Microbial community composition is unaffected by anode potential." *Environ Sci Tech* 48 (2014): 1352-1358.
13. Finkelstein, David A, Leonard M Tender, and J Gregory Zeikus. "Effect of electrode potential on electrode-reducing microbiota." *EnvironSci Tech* 40 (2006): 6990-6995.

14. Parot, Sandrine, Marie-Line Délia, and Alain Bergel. "Forming electrochemically active biofilms from garden compost under chronoamperometry." *Bioresour Tech* 99 (2008): 4809-4816.
15. Mohamed, Abdelrhman, Phuc T Ha, Brent M Peyton, and Rebecca Mueller, et al. "*In situ* enrichment of microbial communities on polarized electrodes deployed in alkaline hot springs." *J Power Sour* 414 (2019): 547-556.
16. Ishii, Shun'ichi, Shino Suzuki, Trina M Norden-Krichmar, and Aaron Tenney, et al. Nealson, and OriannaBretschger. "A novel metatranscriptomic approach to identify gene expression dynamics during extracellular electron transfer." *Nat Comm* 4 (2013): 1-10.
17. Paitier, Agathe, AlexianeGodain, Delina Lyon, and NaoufelHaddour, et al. "Microbial fuel cell anodic microbial population dynamics during MFC start-up." *Biosensors Bioelect* 92 (2017): 357-363.
18. Holmes, De, Dr Bond, RA O'Neil, and CE Reimers, et al. "Microbial communities associated with electrodes harvesting electricity from a variety of aquatic sediments." *Micro Ecol* 482 (2004): 178-190.
19. Daghio, Matteo, Isabella Gandolfi, Giuseppina Bestetti, and Andrea Franzetti, et al. "Anodic and cathodic microbial communities in single chamber microbial fuel cells." *New Biotech* 32 (2015): 79-84.
20. Yates, Matthew D, Patrick D Kiely, Douglas F Call, and Hamid Rismani-Yazdi, et al. "Convergent development of anodic bacterial communities in microbial fuel cells." *The ISMEJ* 6 (2012): 2002-2013.
21. Ieropoulos, Ioannis, Jonathan Winfield, and John Greenman. "Effects of flow-rate, inoculum and time on the internal resistance of microbial fuel cells." *Bioresou Tech* 101 (2010): 3520-3525.
22. Philips, J, K Verbeeck, K Rabaey, and JBAArends. "Ghent University, Gent, Belgium." *Microbial Electrochem Fuel Cells: Fundam App* (2015): 67.
23. Khater, Dena Z, KM El-Khatib, and Helmy M Hassan. "Microbial diversity structure in acetate single chamber microbial fuel cell for electricity generation." *J Gen Eng Biotech* 15 (2017): 127-137.
24. Lee, Jiyoung, Nguyet Thu Phung, In Seop Chang, and Byung Hong Kim, et al. "Use of acetate for enrichment of electrochemically active microorganisms and their 16S rDNA analyses." *FEMSMicrobio Letters* 223 (2003): 185-191.
25. Ishii, Shun'ichi, Shino Suzuki, Trina M Norden-Krichmar, and Tony Phan, et al. "Microbial population and functional dynamics associated with surface potential and carbon metabolism." *The ISME J* 8 (2014): 963-978.
26. Kouzuma, Atsushi, Shun'ichi Ishii, and Kazuya Watanabe. "Metagenomic insights into the ecology and physiology of microbes in bioelectrochemical systems." *Bioresou Tech* 255 (2018): 302-307.
27. Beecroft, Nelli J, Feng Zhao, John R Varcoe, and Robert CT Slade, et al. "Dynamic changes in the microbial community composition in microbial fuel cells fed with sucrose." *App Microbio Biotech* 93 (2012): 423-437.
28. Poretsky, Rachel, Luis M Rodriguez-R, Chengwei Luo, and Despina Tsementzi, et al. "Strengths and limitations of 16SrRNA gene amplicon sequencing in revealing temporal microbial community dynamics." *PloS one* 9 (2014).
29. Rosselli, Riccardo, OttaviaRomoli, Nicola Vitulo, and Alessandro Vezzi, et al. "Direct 16SrRNA-seq from bacterial communities: a PCR-independent approach to simultaneously assess microbial diversity and functional activity potential of each taxon." *Sci Reports* 6 (2016): 32165.
30. Ishii, Shun'ichi, Shino Suzuki, Aaron Tenney, and Kenneth H Nealson, et al. "Comparative metatranscriptomics reveals extracellular electron transfer pathways conferring microbial adaptivity to surface redox potential changes." *The ISME J* 12 (2018): 2844-2863.
31. Bond, Daniel R, Dawn E Holmes, Leonard M Tender, and Derek R Lovley. "Electrode-reducing microorganisms that harvest energy from marine sediments." *Sci* 295 (2002): 483-485.
32. Bond, Daniel R, and Derek R Lovley. "Electricity production by *Geobacter* sulfurreducensattached to electrodes." *Appl Environ Microbiol* 69 (2003): 1548-1555.
33. Fedorovich, Viatcheslav, Matthew C Knighton, Eulyn Pagaling, and F Bruce Ward, et al. "Novel electrochemically active bacterium phylogenetically related to Arcobacterbutzleri, isolated from a microbial fuel cell." *Appl Environ Microbiol* 75 (2009): 7326-7334.
34. Borole, Abhijeet P, Gemma Reguera, Bradley Ringeisen, and Zhi-Wu Wang, et al. "Electroactive biofilms: current status and future research needs." *Energy Environ Sci* 4 (2011): 4813-4834.
35. Fischer, ER, Hansen BT, Nair V, and Hoyt FH, et al. "Scanning Electron Microscopy." *Curr Protocols Microbio* (2012) pp: 1–16.
36. Orakov, Askarbek N, Nazgul K Sakenova, Anatoly Sorokin, and Igor I Goryanin. "ASAR: visual analysis of metagenomes in R." *Bioinform* 34 (2018): 1404-1405.
37. Menzel, Peter, Kim Lee Ng, and Anders Krogh. "Kaiju: Fast and sensitive taxonomic classification for metagenomics." *Biorxiv* (2015): 031229.
38. Westbrook, Anthony, Jordan Ramsdell, TarunaSchuelke, and Louisa Normington, et al. "PALADIN: protein alignment for functional profiling whole metagenome shotgun data." *Bioinform* 33 (2017): 1473-1478.
39. Van den Boogaart, K, Tolosana R, and Bren M. " Compositions: Compositional data analysis." 1 (2018): 40-1.
40. Van den Boogaart, K Gerald, and R Tolosana-Delgado. ""Compositions": a unified R package to analyze compositional data." *Comp Geosci* 34 (2008): 320-338.
41. Anderson, Marti J. "A new method for nonparametric multivariate analysis of variance." *Austral Ecol* 26 (2001): 32-46.
42. Brooks, J Paul, David J Edwards, Michael D Harwich, and Maria C Rivera, et al. "The truth about metagenomics: quantifying and counteracting bias in 16SrRNA studies." *BMC Microbio* 15 (2015): 66.
43. Cord-Ruwisch, Ralf, Derek R Lovley, and Bernhard Schink. "Growth of *Geobacter* sulfurreducenswith acetate in syntrophic cooperation with hydrogen-oxidizing anaerobic partners." *Appl Environ Microbiol* 64 (1998): 2232-2236.
44. Dupuis, Alain, André Peinnequin, Elisabeth Darrouzet, and JoëlLunardi. "Genetic disruption of the respiratory NADH-ubiquinone reductase of Rhodobactercapsulatus leads to an unexpected photosynthesis-negative phenotype." *FEMS Microbiology Letters* 148 (1997): 107-114.
45. Orellana, Roberto. "Physiological models of *Geobacter* sulfurreducensand Desulfobacterpostgatei to understand uranium remediation in subsurface systems." (2014).
46. Oksanen, J, Blanchet FG,Friendly M, and Kindt R, et al. "Vegan:Community Ecology Package." (2019). https://CRAN.R-project.org/package=vegan.
47. Team, R Core. "R: A language and environment for statistical computing." (2013): 201.
48. Shrestha, Pravin Malla, and Amelia-Elena Rotaru. "Plugging in or going wireless: strategies for interspecies electron transfer." *Frontiers Microbio* 5 (2014): 237.
49. Wickham, Hadley. "Ggplot2: Elegant graphics for data analysis." *Springer* (2016).
50. Neue, Heinz-Ulrich. "Methane emission from rice fields." *Biosci* 43 (1993): 466-474.
51. Doyle, Lucinda E, Pui Yi Yung, Sumitra D Mitra, and Stefan Wuertz, et al. "Electrochemical and genomic analysis of novel electroactive isolates obtained via potentiostatic enrichment from tropical sediment." *J Power Sour* 356 (2017): 539-548.
52. Pinto, RP, B Srinivasan, MF Manuel, and B Tartakovsky. "A two-population bio-electrochemical model of a microbial fuel cell." *BioresouTech* 101 (2010): 5256-5265.
53. Pasternak, Grzegorz, John Greenman, and Ioannisleropoulos. "Dynamic evolution of anodic biofilm when maturing under different external resistive

loads in microbial fuel cells. Electrochemical perspective." *J Power Sourc* 400 (2018): 392-401.

54. Kim, HyungJoo, Moon Sik Hyun, In Seop Chang, and Byung Hong Kim. "A microbial fuel cell type lactate biosensor using a metal-reducing bacterium, Shewanellaputrefaciens." *J Microbio Biotech* 9 (1999): 365-367.
55. Pinchuk, Grigory E, Dmitry A Rodionov, Chen Yang, and Xiaoqing Li, et al. "Genomic reconstruction of Shewanellaoneidensis MR-1 metabolism reveals a previously uncharacterized machinery for lactate utilization." *Proceedings of the National Academy of Sci* 106 (2009): 2874-2879.
56. Ishii, Yoshikazu, Morio Miyahara, and Kazuya Watanabe. "Anode macrostructures influence electricity generation in microbial fuel cells for wastewater treatment." *J BiosciBioeng* 123 (2017): 91-95.
57. Gregory, Kelvin B, Daniel R Bond, and Derek R Lovley. "Graphite electrodes as electron donors for anaerobic respiration." *EnvironMicrobio* 6 (2004): 596-604.
58. Lovley, Derek R. "Syntrophy goes electric: direct interspecies electron transfer." *Ann Rev Microbio* 71 (2017): 643-664.
59. Shrestha, Pravin Malla, Amelia-Elena Rotaru, Zarath M Summers, and Minita Shrestha, et al. "Transcriptomic and genetic analysis of direct interspecies electron transfer." *Appl Environ Microbiol* 79 (2013): 2397-2404.
60. Steimle, Stefan, CsabaBajzath, Katerina Dörner, and Marius Schulte, et al. "Role of subunit NuoL for proton translocation by respiratory complex I." *Biochem* 50 (2011): 3386-3393.
61. McCallum, Matthew, Stephanie Tammam, Ahmad Khan, and Lori L Burrows, et al. "The molecular mechanism of the type IVa pilus motors." *Nat Comm* 8 (2017): 1-10.
62. Steidl, Rebecca J, SanelaLampa-Pastirk, and Gemma Reguera. "Mechanistic stratification in electroactive biofilms of *Geobacter* sulfurreducensmediated by pilus nanowires." *Nat Comm* 7 (2016): 12217.
63. Butler, Jessica E, Nelson D Young, and Derek R Lovley. "Evolution of electron transfer out of the cell: comparative genomics of six *Geobacter* genomes." *BMC Gen* 11 (2010): 40.
64. Levar, Caleb E, Colleen L Hoffman, Aubrey J Dunshee, and Brandy M Toner, et al. "Redox potential as a master variable controlling pathways of metal reduction by *Geobacter* sulfurreducens." *The ISME J* 11 (2017): 741-752.
65. Conover, William J, and Ronald L Iman. "Analysis of covariance using the rank transformation." *Biometrics* (1982): 715-724.
66. Quade, Dana. "Rank analysis of covariance." *J Amer Stat Assoc* 62 (1967): 1187-1200.
67. Saeedghalati, Mohammadkarim, FarnoushFarahpour, Bettina Budeus, and Anja Lange, et al. "Quantitative comparison of abundance structures of generalized communities: from B-cell receptor repertoires to microbiomes." *PLoS Comput Biol* 13 (2017): e1005362.
68. Doyle, Lucinda E, and Enrico Marsili. "Weak electricigens: A new avenue for bioelectrochemical research." *Bioresour Tech* 258 (2018): 354-364.

How to cite this article: Lukasz Szydlowski, Sorokin Anatoly, Vasieva Olga, and Boerner Susan, et al. "Evolutionary Dynamics of Microbial Communities in Bioelectrochemical Systems". J Comput Sci Syst Biol 13 (2020) doi: 10.37421/jcsb.2020.13.310